Reoxygenation Reverses Hypoxic Pulmonary Arterial Remodeling by Inducing Smooth Muscle Cell Apoptosis via Reactive Oxygen Species–Mediated Mitochondrial Dysfunction

Jian Chen, MM; Yan-Xia Wang, MD; Ming-Qing Dong, MD, PhD; Bo Zhang, MD; Ying Luo, MD; Wen Niu, MD; Zhi-Chao Li, MD, PhD

Background—Pulmonary arterial remodeling, a main characteristic of hypoxic pulmonary hypertension, can gradually reverse once oxygen has been restored. Previous studies documented that apoptosis increased markedly during the reversal of remodeled pulmonary arteries, but the types of cells and mechanisms related to the apoptosis have remained elusive. This study aimed to determine whether pulmonary artery smooth muscle cell (PASMC)-specific apoptosis was involved in the reoxygenation-induced reversal of hypoxic pulmonary arterial remodeling and elucidate the underlying mechanism.

Methods and Results—Hypoxic pulmonary hypertension was induced in adult male Sprague–Dawley rats (n=6/group) by chronic hypobaric hypoxia. and the hypoxic pulmonary hypertension rats were then transferred to a normoxia condition. During reoxygenation, hypoxia-induced pulmonary arterial remodeling gradually reversed. The reversal of remodeled pulmonary arteries was associated with increased H_2O_2 and with changes in lung expression of cleaved caspase3/PARP, Bax, and Bcl-2, consistent with increased apoptosis. The PASMC apoptosis, in particular, increased remarkably during this reversal. In vitro, reoxygenation induced the apoptosis of cultured rat primary PASMCs accompanied by increased mitochondrial reactive oxygen species, mitochondrial dysfunction, and the release of cytochrome C from mitochondria to cytoplasm. Clearance of reactive oxygen species alleviated mitochondrial dysfunction as well as the release of cytochrome C and, finally, decreased PASMC apoptosis.

Conclusions—Reoxygenation-induced apoptosis of PASMCs is implicated in the reversal of hypoxic pulmonary arterial remodeling, which may be attributed to the mitochondrial reactive oxygen species–mediated mitochondrial dysfunction. (***J Am Heart Assoc***. 2017;6:e005602. DOI: 10.1161/JAHA.117.005602.)

Key Words: apoptosis • hypoxia • mitochondria • pulmonary hypertension • reoxygenation

Hypoxic pulmonary hypertension (HPH), resulting from chronic lung diseases or occurring as an idiopathic case at high altitude, is a complicated disorder with high morbidity and mortality in adults and neonates.[1-4] Hypoxia generally gives rise to pulmonary vasoconstriction and vascular remodeling.[5] Pulmonary arterial remodeling, due to excessive proliferation or apoptosis resistance of the resident cells in peripheral pulmonary arteries, is a central feature of HPH.[6-9]

From the Department of Pathology and Pathophysiology, Fourth Military Medical University, Xi'an, China.

Correspondence to: Zhi-Chao Li, MD, PhD, Department of Pathology and Pathophysiology, Fourth Military Medical University, Changle West Road 169, Xi'an 710032, China. E-mail: lizhic@fmmu.edu.cn

Intriguingly, previous studies have constantly reported that remodeled pulmonary arteries of established HPH gradually regressed after withdrawal of the hypoxia stimulus.[9-13] However, the mechanism contributing to this reversal is still unclear.

Apoptosis, a well-studied programmed cell death, is critical for tissue development and homeostasis.[14] Therefore, the fluctuation of apoptosis level under different conditions may lead to serious diseases or outcome of them.[15] A study has shown that apoptosis increased remarkably in the reversal of hypoxic pulmonary arterial remodeling after reoxygenation,[12] but the major cells involved in this process were not carefully defined. As is well known, excessive proliferation and apoptosis resistance of pulmonary artery smooth muscle cells (PASMCs) in small pulmonary arteries could cause pulmonary arterial remodeling under hypoxia,[16] yet during reoxygenation, the thickened medial layer could gradually reverse.[11,13] More importantly, previous studies indicated that inducing PASMC apoptosis could prevent and reverse

<div style="border:1px solid red">

Clinical Perspective

What Is New?

- Increased apoptosis of pulmonary artery smooth muscle cells participates in the reoxygenation-induced reversal of hypoxic pulmonary arterial remodeling, which may be triggered by mitochondrial reactive oxygen species–mediated mitochondrial dysfunction.

What Are the Clinical Implications?

- This study suggests that reoxygenation initiates pulmonary artery smooth muscle cell apoptosis during reversal of pulmonary arterial remodeling in hypoxic pulmonary hypertension rats. Further studies may be needed to delineate the effect of correcting hypoxia on pulmonary artery remodeling in secondary pulmonary hypertension associated with chronic obstructive pulmonary disease.
- This would shed light on the therapeutic potential of supplemental oxygen in hypoxic pulmonary hypertension.

</div>

established pulmonary vascular remodeling.[17-19] However, whether increased apoptosis of PASMCs participated in the reversal of pulmonary arterial remodeling during reoxygenation has not been clarified.

As an evolutionarily conserved process, apoptosis can be initiated by intrinsic (reactive oxygen species [ROS] or DNA and mitochondrial damage) or extrinsic (ligand of death receptors) factors,[20] among which, ROS arising from cytoplasm or mitochondria is high profile.[21-23] Generally, there is a destructive ROS burst during the early reoxygenation following hypoxia,[24] which can lead to damage to macromolecules and organelles.[25,26] For example, large amounts of ROS can be produced during myocardial ischemia-reperfusion (hypoxia-reoxygenation) injury, subsequently giving rise to the apoptosis of myocardium and heart failure.[27] Not only the major site of ROS production, mitochondria are also a susceptible target of ROS for deleterious effects.[28] Ordinarily, excessive ROS could rapidly raise the permeability of the inner mitochondrial membrane, known as the mitochondrial permeability transition, resulting in the depolarization of mitochondrial potential. Alternatively, the increased ROS could disturb the balance of Bcl-2-like antiapoptotic factors and Bax-like proapoptotic factors of Bcl-2 family proteins. These 2 changes finally result in mitochondrial outer membrane permeabilization and the release of proapoptotic proteins in the intermembrane space, for example cytochrome C.[21,29] Nevertheless, whether large amounts of ROS are generated and give rise to mitochondria-dependent apoptosis of PASMCs following hypoxia-reoxygenation is still unknown.

This study investigated the effect of PASMC apoptosis in the reversal of hypoxic pulmonary remodeling and its possible

mechanism during reoxygenation. The results suggest that during reoxygenation, the increased apoptosis of PASMCs participates in the reversal of hypoxic pulmonary arterial remodeling. Moreover, reoxygenation-induced mitochondrial ROS results in mitochondrial dysfunction, which may be involved in the mechanism of the increased apoptosis of PASMCs.

Materials and Methods

Animal Experiments

All animal procedures were approved by the Animal Care and Use Committee of the Fourth Military Medical University and performed in accordance with the National Institutes of Health Guide for the Care and Use of Laboratory Animals. First, adult male Sprague–Dawley rats were randomly divided into 4 groups: (1) normoxia for 4 weeks (group N), n=6; (2) hypoxia for 4 weeks (group H), n=6; (3) reoxygenation for 1 week after hypoxia for 4 weeks (group R1), n=6; and (4) reoxygenation for 6 weeks after hypoxia for 4 weeks (group R6), n=6. To further explore the effect of ROS on the reversal of hypoxic pulmonary arterial remodeling, rats were randomly divided into 5 groups: (1) N, n=6; (2) H, n=6; (3) R1, n=6; (4) R1+MitoTEMPO, n=6; and (5) R1+saline, n=6. Rats in group H were intermittently housed in a hypobaric hypoxia chamber, with fractional inspired oxygen (FiO_2) 0.10, 8 h/d for 4 weeks.[30] Rats in groups R1 and R6 were first exposed to hypoxia for 4 weeks and then transferred to normoxia environment (FiO_2 0.21) for 1 week and 6 weeks, respectively. Rats in R1+MitoTEMPO and R1+saline groups were pretreated with MitoTEMPO (0.7 mg/kg) and phosphate-buffered saline for 3 days before being transferred to the normoxia condition by intraperitoneal injection twice a day, and the treatment continued for another week after the 2 groups were transferred to normoxia. Rats in group N were maintained in normal environment close to the hypoxic chamber for 4 weeks. All animals were kept in individual ventilated cages, which were placed in a 12:12 light-dark cyclic and temperature-controlled room.

Hemodynamic Measurements and Tissues Preparation

At the end of interventions all rats were fasted overnight (12 hours) and then anesthetized with 20% urethane (4 mL/kg) through intraperitoneal injection. During the experiment, animal temperature, respiration, and heart rates remained stable as verified by continuous monitoring. A soft catheter linked to a pressure transducer was inserted into the right ventricle through the right external jugular vein. Right ventricle systolic pressure (RVSP), approximately equal to

pulmonary arterial pressure,[31,32] was recorded on the monitor of the Powerlab system (AD Instruments, Castle Hill, New South Wales, Australia). Systemic systolic pressure was measured through a catheter inserted into the carotid artery. After measurements, rats were immediately exsanguinated, and hearts as well as lungs were removed. Right lower lobes were fixed in 4% paraformaldehyde, and the remaining lung tissues were stored in liquid nitrogen for further analysis. To evaluate the degree of right ventricle (RV) hypertrophy, the RV free wall was sliced from the left ventricle (LV) plus septum (Sep) and weighed. Right ventricle hypertrophy was assessed through the ratio RV/(LV+Sep).

Vascular Morphometry

To investigate the morphological changes of pulmonary arteries, the paraffin sections of peripheral rat lungs were stained with hematoxylin and eosin. Peripheral pulmonary arteries (30 to 100 µm in diameter, 10 vessels/section), running along the terminal and respiratory bronchioles as well as alveolar duct, were randomly collected through digital photomicrograph (Leica, Heidelberg, Germany). The percentage medial layer thickness (MT%=100×[medial layer thickness]/[vessel semidiameter]) and area (MA%=100×[cross-sectional medial layer area]/[total cross-sectional vessel area]) of peripheral pulmonary arteries were analyzed in a blinded method using an image-processing program (Image-Pro Plus, Version 6.0, Media Cybernetics, Rockville, MD).

Measurement of H_2O_2 in Lungs

The amount of H_2O_2 in fresh lung tissues was immediately examined using a commercially available Hydrogen Peroxide Assay Kit (Beyotime Inc, Jiangsu, China) according to the recommended protocols. The concentrations of H_2O_2 in different groups were finally normalized to the corresponding protein concentrations.

Immunohistochemistry

Tissue sections were dewaxed and rehydrated in xylene and ethanol solutions. Endogenous peroxidase was blocked by hydrogen peroxide. Antigen retrieval of these sections was performed in a 0.4 mol/L sodium citrate buffer through microwave after incubation with cleaved-caspase3 (1:100; Cell Signaling Technology, Danvers, MA), Bax, Bcl-2 (1:50, Boster, Wuhan, China), LC3 (1:50, Millipore, Billerica, MA), P62 (1:100, Sigma, St. Louis, MO), RIP, and smooth muscle α-actin (1:100, Abcam, Cambridge, UK) at 4°C overnight. All sections were labeled by goat antirabbit antibody (ZSGB-BIO, Beijing, China) and visualized using a DAB Kit (ZSGB-BIO,

Beijing, China). The immunoreactivity in the pulmonary arterial medial layer was analyzed in a blinded method using an image-processing program (Image-Pro Plus, Version 6.0, Media Cybernetics, Rockville, MD).

Terminal Deoxynucleotidyl Transferase dUTP Nick-End Labeling Assay

Apoptosis in the peripheral pulmonary arteries was detected using an In Situ Cell Death Detection Kit (Roche, Basel, Switzerland) to label free 3′-OH termini with modified nucleotides in an enzymatic reaction. After being dewaxed and hydrated, tissue sections were processed following the manufacturer's instructions. Fluorescent signals were then recorded by fluorescence microscope (Leica, Heidelberg, Germany). The apoptosis level was evaluated through the number of terminal deoxynucleotidyl transferase dUTP nick-end labeling–positive nuclei per vessel of different groups.[33]

Cell Culture

Rat primary PASMCs were prepared through a tissue explant method.[34] The methods of anesthesia and euthanasia were in accordance with those described above. Pulmonary arteries were isolated from rats, and adventitial as well as intimal layers were gently removed. The remaining media was dissected into small pieces and spread on the bottom of culture flask. Dulbecco Eagle's minimum essential medium (HyClone, Logan, UT) with 20% fetal bovine serum (CellMax, Beijing, China) was added into the flask. The culture flask was placed upside down in a 37°C, 5% CO_2 humidified incubator and turned over 3 hours later. PASMCs began to climb out after 3 days. The purity and identity were verified through immunocytochemical staining against smooth muscle α-actin. PASMCs were utilized from passages 3 to 5.

MTT Assay

PASMCs were seeded in 96-well plates and quiesced in serum-free medium for 24 hours after growing to subconfluence. To investigate the hypoxia-induced growth, PASMCs ($6×10^3$ cells/well) were exposed to 5% oxygen for 0, 24, 36, 48, 60, and 72 hours with normoxia being utilized on controls. To further explore the growth of PASMCs during reoxygenation, PASMCs ($3×10^3$ cells/well) were first exposed to hypoxia for 48 hours and then transferred to normoxia for 0, 24, 36, and 48 hours (H48R0, H48R24, H48R36, and H48R48) with normoxia being utilized as control (N48, N72, N84, and N96). At each end point, MTT was added into the plates (5 mg/mL, 20 µL/well) and

incubated for another 4 hours. Dimethyl sulfoxide was added into each well, and all plates were shaken for 10 minutes in a shaker. The optical density (OD) values were collected using a spectrophotometer (PowerWave XS, BioTek Inc, Winooski, VT).

BrdU Incorporation Assay

PASMCs (1.2×10^4 cells) were seeded on coverslips in 24-well plates and quiesced in serum-free medium for 24 hours, when they reached 50% confluence. The proliferation capacity was explored by the incorporation of the thymidine analogue 5-bromo-2′-deoxyuridine into the DNA of proliferating cells according to the recommended protocol of the 5-Bromo-2′-deoxyuridine Labeling and Detection Kit II (Roche, Basel, Switzerland). All cells were counterstained with nuclear fast red and observed under a light microscope. PASMC proliferation was assessed by the percentage of BrdU-positive nuclei.[35]

Flow Cytometry

At the end of all interventions, PASMCs ($>1 \times 10^6$ cells) were collected and stained with Annexin V-FITC/propidium iodide Kit (Roche, Basel, Switzerland) according to the manufacturer's protocol. The apoptosis of PASMCs was measured by a Coulter Epics XL-MCL™ Flow Cytometer (Beckman Coulter, Inc, Indianapolis, IN).

Measurement of ROS

PASMCs in N72, H48R24, H48R24+NAC (10 mmol/L, a nonspecific ROS inhibitor, Sigma-Aldrich, St. Louis, MO), and H48R24+MitoTEMPO (1 μmol/L, a mitochondrial-targeted antioxidant; Santa Cruz Biotechnology, Dallas, TX) groups were stained with an oxidant-sensitive fluorescence dye DCFH-DA (10 μmol/L, Nanjing Jiancheng Bioengineering Institute, Nanjing, China) and a mitochondria-specific fluorogenic probe MitoSOX Red (5 μmol/L, Invitrogen, Carlsbad, CA). Subsequently, the intracellular total ROS and mitochondrial ROS were detected through fluorescence microscopy (Leica, Heidelberg, Germany) and flow cytometry, respectively.

Moreover, isolated mitochondria (30 μg protein) from N72, H48R24, H48R24+NAC, and H48R24+MitoTEMPO groups were added into microplate wells containing respiration buffer (5 mmol/L pyruvate, 2.5 mmol/L malate) and 10 μmol/L DCFH-DA.[36] After incubation for 10 minutes at 37°C, the fluorescence was measured using Fluoroskan Ascent™ FL (Thermo Fisher Scientific, Waltham, MA) with an excitation wavelength of 500 nm and emission wavelength of 525 nm.

Western Blotting

Lung tissues and cultured rat primary PASMCs were lysed in RIPA lysis buffer (Beyotime Inc, Jiangsu, China) containing 0.2 mmol/L phenylmethanesulfonyl fluoride. Lysate solutions were centrifuged at 12 000 rpm ($\times 14000$ g) for 20 minutes, and supernatant was collected. The protein concentrations were determined using a BCA protein assay kit (Beyotime Inc, Jiangsu, China). The protein suspensions of different groups, containing equal amounts of proteins (30 μg), were separated by SDS-PAGE, transferred to polyvinylidene fluoride membrane (Millipore, Billerica, MA) and blocked with 5% milk solution. Membranes were incubated with the solutions of cleaved caspase3/poly-ADP ribose polymerase (PARP), Bcl-2, Bax, proliferating cell nuclear antigen, and COX-IV (1:800, Cell Signaling Technology, Danvers, MA) and β-actin (1:2000, ImmunoWay, Plano, TX) at 4°C overnight. To measure the release of cytochrome C, the mitochondrial and cytosol pellets were isolated and immunoblotted by antibodies against cytochrome C (1:800, Cell Signaling Technology, Danvers, MA) with voltage-deopendent anion channel (1:800; Cell Signaling Technology) and β-actin serving as controls. Blots were then probed by an enhanced chemiluminescence reagent (Millipore, Billerica, MA) after incubation with the corresponding horseradish-peroxidase-conjugated antibody solution.

Estimation of Mitochondrial Membrane Potential

To explore the apoptosis mechanism, PASMCs (1.2×10^4 cells) were seeded on the coverslips and stained with JC-1 (GeneCopoeia, Rockville, MD), a potential-dependent cationic dye, at 10 μg/mL for 20 minutes in the dark. Intracellular distribution of JC-1 was measured through a confocal microscope, and the red/green fluorescence ratios were calculated through an image-processing program (Image-Pro Plus, Version 6.0; Media Cybernetics, Rockville, MD).[37]

Determination of Mitochondrial ATP

Mitochondrial ATP production was measured using an ATP Determination Kit (Invitrogen, Carlsbad, CA) according to the manufacturer's instructions. Isolated mitochondria (5 μg) were added into 100 μL reaction buffer and incubated for 15 minutes.[36] The luminescence was then measured by Fluoroskan Ascent™ FL. Mitochondrial ATP production was relatively calculated by the intensity of luminescence.

Statistical Analysis

Data were presented as means±SEM. The statistical differences were analyzed by the Student's t test or 1-way ANOVA followed by the Bonferroni posttest using GraphPad Prism 5.0

software (GraphPad Software Corp, San Diego, CA). $P<0.05$ was considered statistically significant.

Results

Hypoxic Pulmonary Arterial Remodeling, Especially the Thickened Medial Layers, Gradually Reversed Following Reoxygenation

Four weeks after exposure to hypoxia, RVSP (Figure 1A), right ventricle hypertrophy (Figure 1F), MT% (Figure 1B through D) and MA% (Figure 1E) of HPH rats increased significantly, compared with the normoxia group. To determine whether the established pulmonary arterial remodeling of HPH rats was reversible, all rats were transferred to normoxia condition after hypoxic exposure. According to the hematoxylin eosin staining, MT% and MA%, 2 key indicators of pulmonary arterial remodeling, reversed significantly during reoxygenation compared with hypoxia group (Figure 1D and 1E). The increased RVSP (Figure 1A) and RV hypertrophy (Figure 1F) also reduced during reoxygenation. Neither hypoxia nor reoxygenation had an obvious effect on systemic systolic pressure (Figure 1G).

Reoxygenation Reversed Hypoxia-Induced Apoptosis Resistance as Well as Proliferation and Increased H_2O_2 Production in Lungs

To explore the possible mechanism involved in the reversal of pulmonary arterial remodeling, the levels of apoptosis and proliferation in lung tissues were determined by Western blotting. The expression of Bax (Figure 2A) as well as cleaved caspase3/PARP (Figure 2D and 2E) and the ratio of Bax/Bcl-2 (Figure 2C) decreased remarkably under hypoxia as compared with the normoxia group, which all gradually regressed during reoxygenation. The expression of Bcl-2 increased markedly under hypoxia as compared with the normoxia group (Figure 2B). Following reoxygenation, the Bcl-2 expression gradually decreased compared with the hypoxia group (Figure 2B). The level of proliferating cell nuclear antigen was upregulated under hypoxia as compared with the normoxia group, which decreased during reoxygenation as compared with the hypoxia group (Figure 2F).

To investigate whether the apoptosis of PASMCs was related to the increased ROS during reoxygenation, H_2O_2, a stable ROS, was measured. As shown in Figure 2G, H_2O_2 increased under hypoxia as compared with the normoxia group. Interestingly, compared with the hypoxia group, H_2O_2 further increased during reoxygenation (Figure 2G). All these findings suggested that reoxygenation reversed hypoxia-induced apoptosis resistance and proliferation, which might be associated with increased ROS.

Reoxygenation Induced PASMC Apoptosis of Peripheral Pulmonary Arteries

In view of the obvious reversal of medial layer changes during the reversal of pulmonary arterial remodeling, we then determined whether the reversal of remodeled pulmonary arteries was associated with increased apoptosis of PASMCs by staining for terminal deoxynucleotidyl transferase dUTP nick-end labeling, cleaved-caspase3, BAX, and Bcl-2 in lung sections. After hypoxia exposure, terminal deoxynucleotidyl transferase dUTP nick-end labeling–positive nuclei in pulmonary arterial wall decreased as compared with the normoxia group, which increased significantly during reoxygenation as compared with the normoxia and hypoxia groups (Figure 3A and 3C). The cleaved-caspase3 (Figure 3B and 3D) and Bax (Figure 3E and 3G) staining were absent in the thickened medial layer after hypoxia as compared with the normoxia group, in which they rapidly increased during reoxygenation. The Bcl-2 staining (Figure 3F and 3H) was opposite to that of Bax. These results showed that the apoptosis of PASMCs in peripheral pulmonary arteries increased dramatically during reoxygenation, which might participate in the reversal of hypoxic pulmonary arterial remodeling.

Reoxygenation Did Not Upregulate PASMC Autophagy and Necroptosis in Peripheral Pulmonary Arteries

To further determine whether the other modes of cell death were implicated into the reversal of hypoxic pulmonary arterial remodeling, the autophagy and necroptosis of PASMCs were examined by immunohistochemistry. As compared with normoxia group, hypoxia increased the expression of LC3 and decreased the P62 expression of the medial layer of peripheral pulmonary arteries, which gradually reversed to normoxia level during reoxygenation (Figure 4A and 4B). The expression of RIP had no significant changes during hypoxia and reoxygenation (Figure 4C).

The Growth of Cultured Rat PASMCs Decelerated Following Hypoxia-Reoxygenation In Vitro

We next investigated whether the growth of isolated rat PASMCs would exhibit a similar reversal process to that of remodeled pulmonary arteries following hypoxia-reoxygenation. As shown in Figure 5A, hypoxia (5% O_2) markedly increased the optical density values, correlating positively
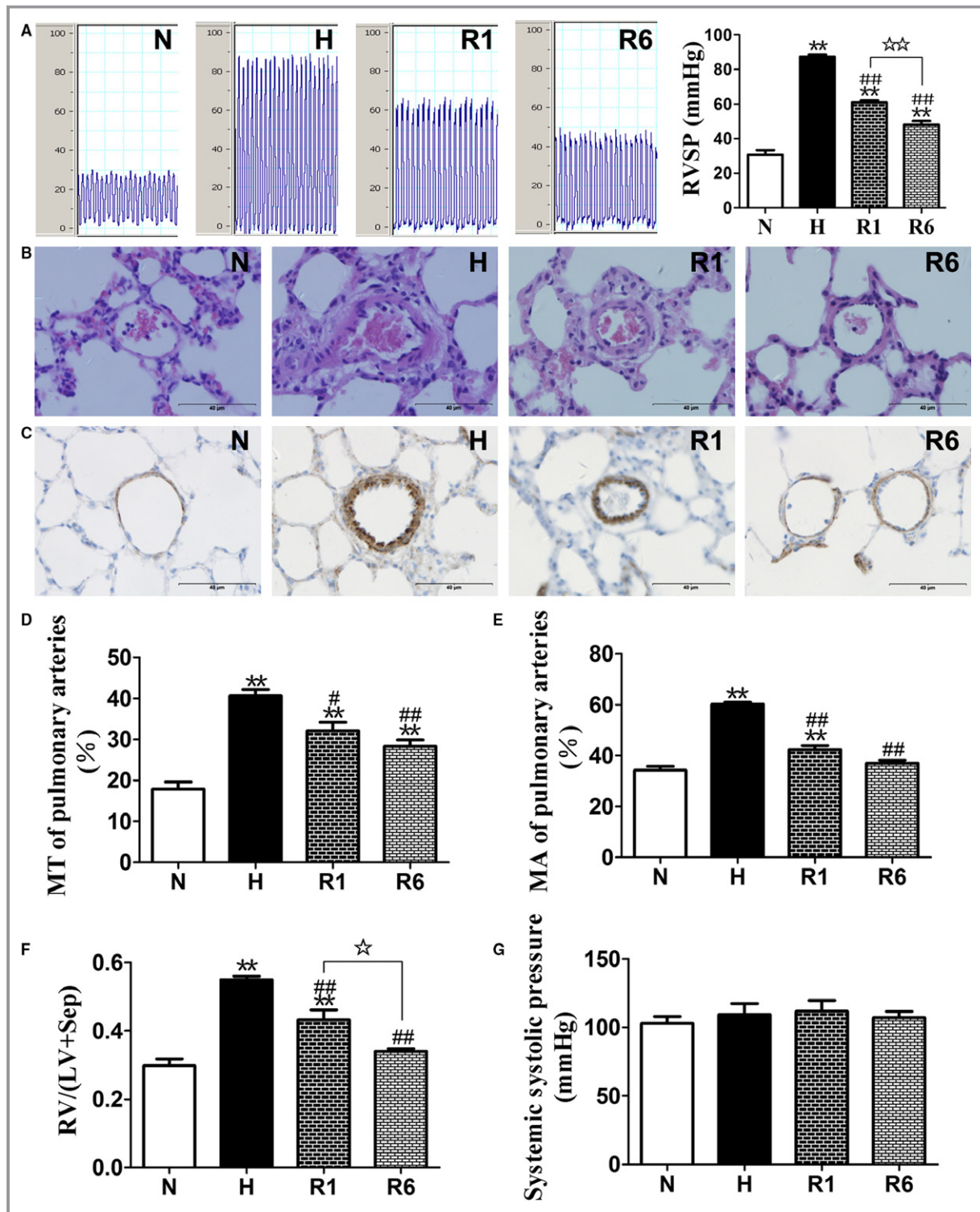
Figure 1. Hypoxic pulmonary arterial remodeling gradually reversed following reoxygenation. Representative images of right ventricle pressure traces and quantitative data of right ventricle systolic pressure (RVSP) are shown (A). The paraffin sections of peripheral rat lungs were analyzed for pulmonary arterial remodeling by hematoxylin eosin staining (B) and immunohistochemical staining against smooth muscle α-actin (C), all at ×400 magnification. Bar, 40 μm. Blinded quantitative analysis of MT% (medial thickness) and MA% (medial area) of peripheral pulmonary arteries (30 vessels/3 sections of an animal, 30 to 100 μm in diameter) was performed with Image-Pro Plus (D and E). (Right ventricle)/(left ventricle+septum) (RV/[LV+Sep]) and systemic systolic pressure are exhibited in bar charts (F and G). Data are presented as means±SEM (n=5-6 animals). **P<0.01 vs normoxia group; #P<0.05, ##P<0.01 vs hypoxia group; *P<0.05, **P<0.01 reoxygenation 1 week vs 6 week by 1-way ANOVA with the Bonferroni posttest. N, normoxia for 4 weeks; H, hypoxia for 4 weeks; R1, reoxygenation for 1 week after hypoxia for 4 weeks; R6, reoxygenation for 6 weeks after hypoxia for 4 weeks.
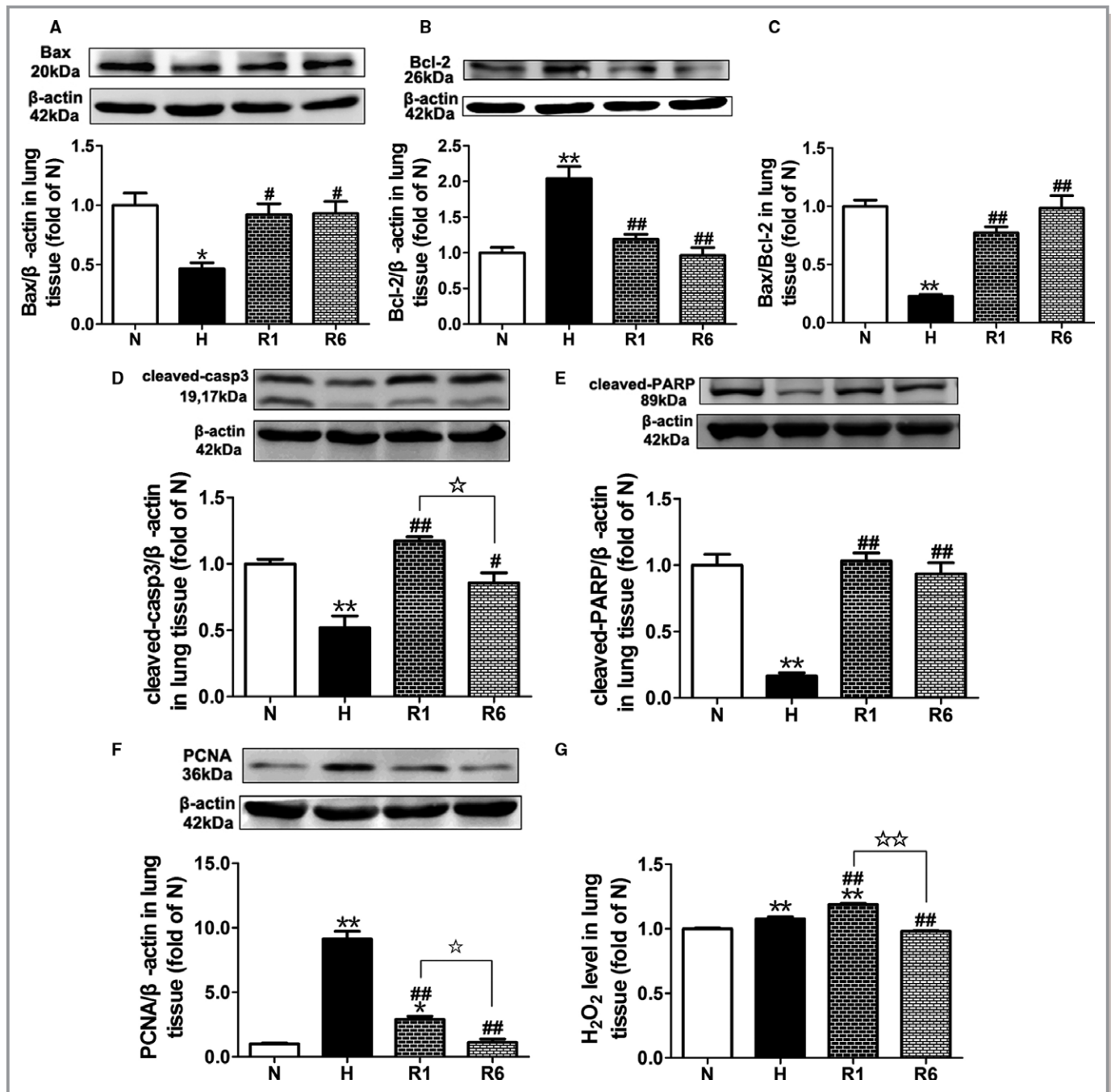
Figure 2. Reoxygenation reversed hypoxia-induced proliferation as well as apoptosis resistance and increased H_2O_2 production in lungs. Western blotting analysis of Bax (A), Bcl-2 (B), cleaved caspase3 (D), cleaved-PARP (E), and PCNA (F) expressions in rat lungs was performed with β-actin as an internal control. The protein ratio of Bax to Bcl-2 was also calculated (C). H_2O_2 levels in lung tissues were examined (G). Data are normalized to those of the normoxia group and expressed as means±SEM (n=4 independent experiments). *$P<0.05$, **$P<0.01$ vs normoxia group; #$P<0.05$, ##$P<0.01$ vs hypoxia group; ☆$P<0.05$, ☆☆$P<0.01$ reoxygenation 1 week vs 6 weeks by 1-way ANOVA with the Bonferroni posttest. PARP indicates poly-ADP ribose polymerase; PCNA, proliferating cell nuclear antigen. N, normoxia for 4 weeks; H, hypoxia for 4 weeks; R1, reoxygenation for 1 week after hypoxia for 4 weeks; R6, reoxygenation for 6 weeks after hypoxia for 4 weeks.

with the number of PASMCs, from 24 hours to 48 hours as compared with normoxia groups. This suggested that hypoxia accelerated the growth of PASMCs, especially at 48 hours, which mimicked the hypoxia-induced remodeling of pulmonary arteries in vitro.

During reoxygenation, the optical density values exhibited a relatively low level as compared with normoxia groups, particularly after reoxygenation for 24 hours (Figure 5B). These findings indicated that the growth of PASMCs exposed to hypoxia first would slow down once reoxygenated.
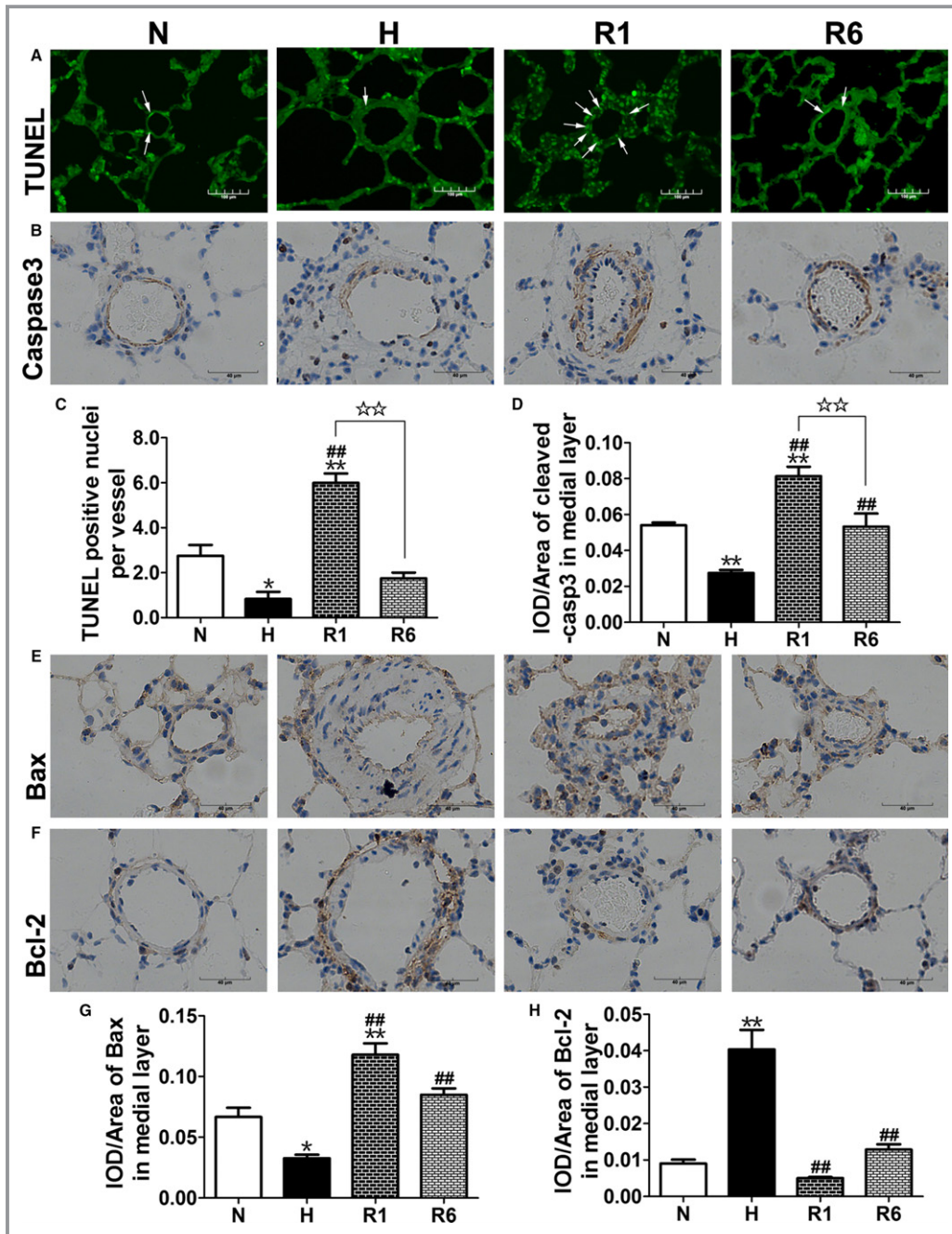
Figure 3. Reoxygenation-induced pulmonary arterial smooth muscle cells (PASMC) apoptosis of periphery pulmonary arteries. Paraffin sections of peripheral rat lungs were subjected to TUNEL analysis (A) and immunostaining for cleaved caspase3 (B), Bax (E), and Bcl-2 (F) to evaluate the apoptosis of PASMCs in pulmonary arterial medial layer (30 to 100 μm in diameter). Representative images of TUNEL at ×200 magnification. Bar, 100 μm. White arrows point to TUNEL-positive nuclei. The images of cleaved caspase3, Bax, and Bcl-2 at ×400 magnification. Bar, 40 μm. Blinded quantitative analysis of the staining was performed. Bar charts showing the number of TUNEL-positive nuclei per vessel (C) and staining density ([integral optical density]/area; IOD/area) of cleaved caspase3 (D), Bax (G), and Bcl-2 (H) of different groups. Data are expressed as means±SEM (n=3-5 animals, 30 vessels/3 sections of an animal). *P<0.05, **P<0.01 vs normoxia group; ##P<0.01 vs hypoxia group; ☆☆P<0.01 reoxygenation 1 week vs 6 weeks by 1-way ANOVA with the Bonferroni posttest. TUNEL indicates terminal deoxynucleotidyl transferase dUTP nick-end labelling. N, normoxia for 4 weeks; H, hypoxia for 4 weeks; R1, reoxygenation for 1 week after hypoxia for 4 weeks; R6, reoxygenation for 6 weeks after hypoxia for 4 weeks.
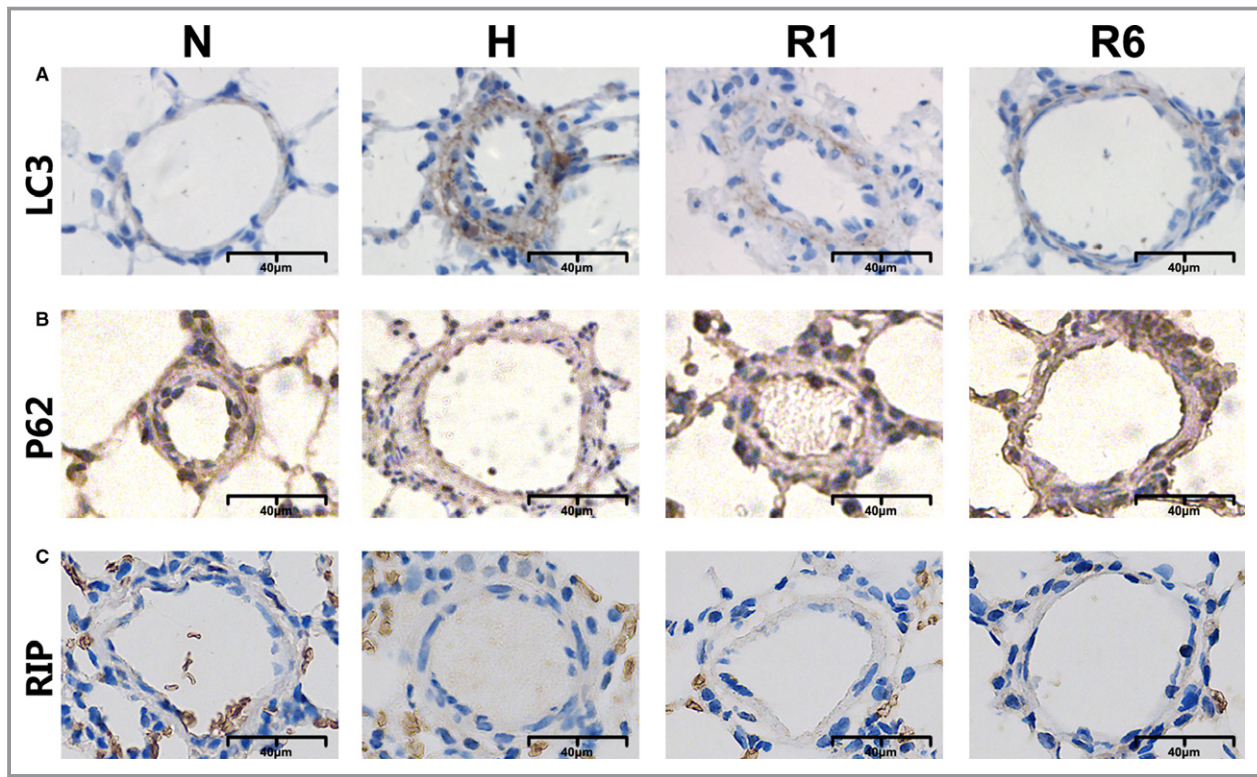
Figure 4. Reoxygenation did not upregulate the pulmonary arterial smooth muscle cells (PASMC) autophagy and necroptosis in peripheral pulmonary arteries. The immunohistochemical staining for LC3, P62, and RIP was performed with the paraffin sections of peripheral rat lungs to evaluate the autophagy and necroptosis of PASMCs in pulmonary arteries (30 to 100 μm in diameter). Representative images of LC3 (A), P62 (B) and RIP (C) at ×400 magnification. Bar, 40 μm. N, normoxia for 4 weeks; H, hypoxia for 4 weeks; R1, reoxygenation for 1 week after hypoxia for 4 weeks; R6, reoxygenation for 6 weeks after hypoxia for 4 weeks.

Increased Apoptosis of Cultured Rat PASMCs Occurred Following Hypoxia-Reoxygenation

Because both increased apoptosis and decreased proliferation could decelerate the growth of PASMCs, we then examined the levels of apoptosis and proliferation of PASMCs during reoxygenation. As evidenced by the Annexin V-FITC/PI analysis, the percentage of apoptotic PASMCs increased dramatically during reoxygenation, compared with normoxia
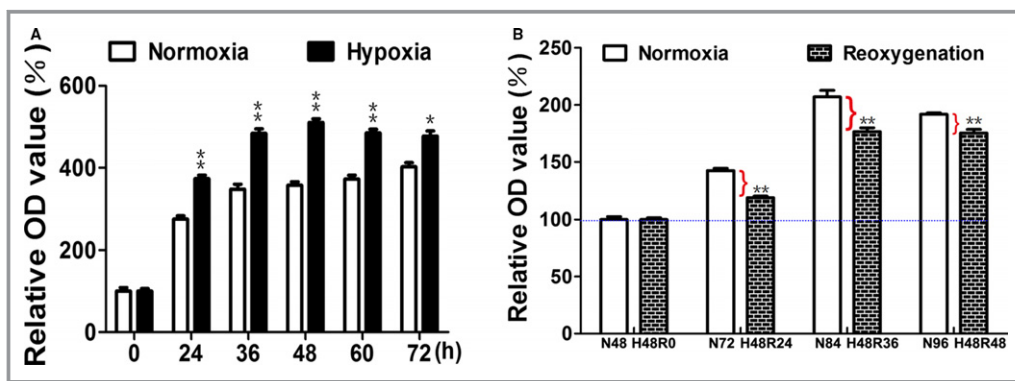

Figure 5. The growth of cultured rat pulmonary arterial smooth muscle cells (PASMCs) decelerated during reoxygenation. PASMCs were exposure to hypoxia (5% O_2) or normoxia (21% O_2) for 0, 24, 36, 48, 60, and 72 hours (A). For reoxygenation study, PASMCs were first exposed to hypoxia for 48 hours and then transferred to normoxia for 0, 24, 36, and 48 hours (B). The growth of PASMC number was measured by MTT assay. Bar charts within the red braces of normoxia groups represent the increased parts of PASMC growth compared to reoxygenation groups. The optical density (OD) values were normalized to control and expressed as means±SEM (n=6-8 wells). *$P<0.05$, **$P<0.01$ vs normoxia group by independent-samples Student t test.
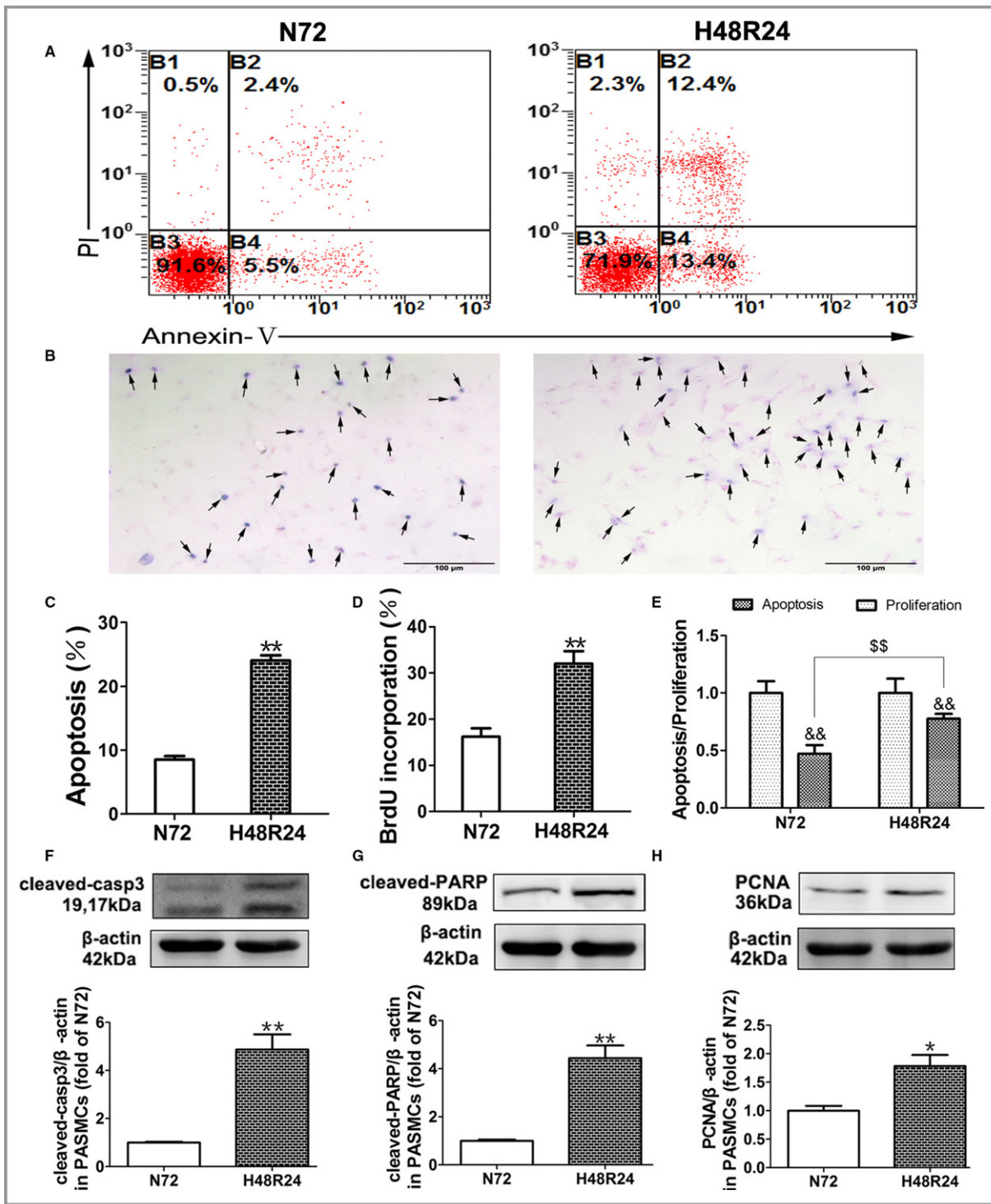
Figure 6. The apoptosis and proliferation of pulmonary arterial smooth muscle cells (PASMCs) increased during reoxygenation in vitro. The apoptosis of PASMCs (>10^6 cells/test) was measured by flow cytometry with Annexin V-FITC/PI staining (A). The proliferation of PASMCs (>2×10^4 cells/coverslip) was determined by BrdU (5-bromo-2′-deoxyuridine) incorporation assay (B). At ×200 magnification; Bar, 100 μm. The black arrows point to the BrdU-positive nuclei. Bar charts showing the percentages of apoptotic cells (C) and BrdU-positive cells (D). The apoptosis was normalized to corresponding proliferation of PASMCs (E). Western blotting analysis of cleaved caspase3 (F), cleaved-PARP (G), and PCNA (H) expressions in PASMCs (>2×10^6 cells/sample) was performed with β-actin as an internal control. Densitometry analysis of protein abundance was conducted by normalizing to that of β-actin. Data are expressed as means ± SEM (n=3-4 independent experiments). *P<0.05, **P<0.01 vs normoxia group; $^{\&\&}$P<0.01 vs corresponding proliferation group; $^{\$\$}$P<0.01 reoxygenation vs normoxia group by independent-samples Student t test. PARP indicates poly-ADP ribose polymerase; PCNA, proliferating cell nuclear antigen.

group (Figure 6A and 6C). The PASMC proliferation also increased during reoxygenation according to the BrdU incorporation assay (Figure 6B and 6D). However, the PASMC apoptosis, normalized to proliferation, increased remarkably during reoxygenation as compared with the normoxia group (Figure 6E). Moreover, the expression of cleaved-caspase3/PARP increased profoundly during reoxygenation (Figure 6F and 6G). The proliferating cell nuclear antigen expression also clearly increased during reoxygenation compared with the normoxia group (Figure 6H). Our results showed that the apoptosis of cultured rat PASMCs increased significantly following hypoxia-reoxygenation.

Mitochondrial ROS Facilitated the Apoptosis of PASMCs Following Hypoxia-Reoxygenation

To explore whether increased ROS caused PASMC apoptosis during reoxygenation, we examined total intracellular and mitochondrial ROS through DCFH-DA and MitoSOX Red assays, respectively. Reoxygenation increased both total intracellular (Figure 7A) and mitochondrial ROS (Figure 7B and 7D) as compared with the normoxia group, which was inhibited to a nearly equivalent extent by NAC and MitoTEMPO. In isolated mitochondria, the production of ROS also increased during reoxygenation, which was inhibited by NAC and MitoTEMPO (Figure 7E). We further investigated the effect of increased ROS on the PASMC apoptosis. Similarly, reoxygenation markedly induced PASMC apoptosis as compared with the normoxia group, which was alleviated by NAC and MitoTEMPO to almost same degree as evidenced by Annexin V-FITC/PI analysis (Figure 7C and 7F). The cleaved-caspase3/PARP expression also increased during reoxygenation as compared with normoxia group, which was inhibited by NAC and MitoTEMPO (Figure 7G and 7H). These results demonstrated that increased mitochondrial ROS initiated PASMC apoptosis during reoxygenation.

Mitochondrial Dysfunction Was Markedly Induced by Mitochondrial ROS Following Hypoxia-Reoxygenation

To further investigate the possible mechanism by which the increased ROS initiated PASMC apoptosis, we assessed the mitochondrial function. Mitochondrial membrane potential decreased dramatically following hypoxia-reoxygenation according to the decreased red/green fluorescence intensity ratio through JC-1 staining, which was equally reversed by NAC and MitoTEMPO (Figure 8A and 8B). According to the expression of COX-IV, the total mitochondrial content had no significant difference between the normoxia and reoxygenation groups; nevertheless, after the interventions of NAC and

MitoTEMPO, it decreased markedly as compared with the reoxygenation group (Figure 8C). Moreover, the production of ATP in isolated mitochondria also decreased markedly during reoxygenation, which was equivalently enhanced by NAC and MitoTEMPO (Figure 8D). The expression of Bax and the protein ratio of Bax/Bcl-2 increased following hypoxia-reoxygenation; however, NAC and MitoTEMPO equivalently inhibited these increases (Figure 9C and 9E). The Bcl-2 expression decreased during reoxygenation, which was also reversed by NAC and MitoTEMPO (Figure 9D). As an important proapoptosis factor in mitochondrial intermembrane space, cytochrome C was obviously released from mitochondria to cytoplasm during reoxygenation as compared with the normoxia group, which was equally inhibited by NAC and MitoTEMPO (Figure 9A and 9B). These findings showed that mitochondrial dysfunction was induced by the mitochondrial ROS following hypoxia-reoxygenation, which triggered the PASMC apoptosis.

The Intervention of MitoTEMPO Failed to Prevent the Reversal of Hypoxic Pulmonary Arterial Remodeling In Vivo

To further consolidate our conclusion in vivo, we assessed the reversal of HPH after the intervention of MitoTEMPO during reoxygenation. Following hypoxia, RVSP (Figure 10A and 10C), right ventricle hypertrophy (Figure 10F), MT% (Figure 10B and 10D), and MA% (Figure 10E) of rats increased significantly as compared with the normoxia group, which reversed remarkably after reoxygenation for 1 week. After the intervention of MitoTEMPO, these parameters did not present any significant differences from the reoxygenation and saline groups. Moreover, as shown in Figure 10G, H_2O_2 increased under hypoxia as compared with the normoxia group, which further increased as compared with the hypoxia group during reoxygenation. However, MitoTEMPO did not effectively eliminate the increased H_2O_2 of the reoxygenation group (Figure 10G).

Discussion

In present study, we showed that reoxygenation-induced apoptosis of PASMCs participated in the reversal of hypoxic pulmonary arterial remodeling of HPH rats, which might arise from the increased ROS. In vitro, the apoptosis of PASMCs also increased significantly following hypoxia-reoxygenation, which was initiated by the mitochondrial ROS-mediated mitochondrial dysfunction. This study exhibits a novel advance for understanding the mechanism of reoxygenation-induced reversal of hypoxic pulmonary arterial remodeling.

As reported by increasing number of studies, pulmonary arterial remodeling of HPH would gradually reverse as hypoxia was withdrew.[38-40] More importantly, considerable evidence
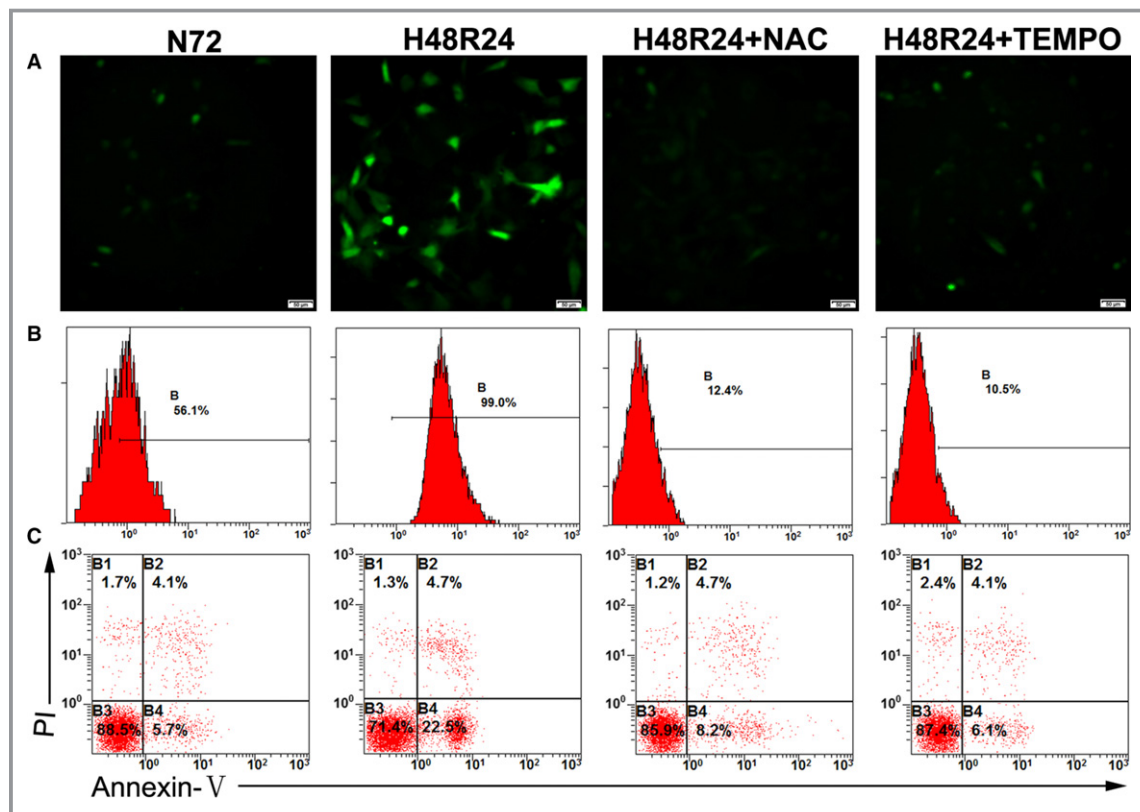
Figure 7. Mitochondrial reactive oxygen species (ROS) facilitated the apoptosis of pulmonary arterial smooth muscle cells (PASMCs) during reoxygenation in vitro. The total ROS in PASMCs ($>2 \times 10^4$ cells/coverslip), in the absence or presence of indicated antioxidants, was detected by fluorescence microscopy after 2,7- dichlorodihydrofluorescein diacetate (DCFH-DA) staining (A). At $\times 200$ magnification; Bar, 50 μm. Flow cytometry analyzes mitochondrial ROS in PASMCs ($>10^6$ cells/test) with fluorescent dye MitoSOX red (B). The percentage of mitochondrial ROS-positive cells is normalized to the normoxia group and expressed as mean±SEM (n=3 independent experiments) (D). Mitochondrial ROS in isolated mitochondria was determined by assessing the fluorescence with the ROS detection dye DCFH-DA (E). The apoptosis of PASMCs ($>10^6$ cells/test) was determined by flow cytometry with Annexin V-FITC/PI staining (C), and the percentage of apoptotic cells is expressed as mean ± SEM (n=3 independent experiments) (F). The expressions of cleaved caspase3 (G) and cleaved PARP (H) were examined by Western blotting. Densitometry analysis of protein abundance was conducted by normalizing to that of β-actin. Data are normalized to the normoxia group and expressed as means±SEM (n=3 independent experiments). *$P<0.05$, **$P<0.01$ vs normoxia group; #$P<0.05$, ##$P<0.01$ vs reoxygenation group by 1-way ANOVA with the Bonferroni posttest.

indicated that the thickened medial layer of HPH regressed most obviously during reoxygenation.[41] The present study showed that the reversal of thickened medial layer played a crucial role in the reversal of hypoxic pulmonary arterial remodeling. During this process, some variables, for example RV/(LV+Sep) and MA, differed between R1 and R6 group. Actually, the level of damage factors couldn't immediately reach up to the threshold of apoptosis of all PASMCs in the peripheral pulmonary arteries during reoxygenation, so the occurrence of apoptosis and clearance of apoptotic PASMCs couldn't complete at the same time, which implied that the reversal of hypoxic pulmonary arterial remodeling might show a sequential feature. Consequently, R1 (as the early stage of reversal) and R6 (as the late stage of reversal) were set to explore the reversal of hypoxic pulmonary arterial remodeling.

Concerning the reversal of pulmonary remodeling, we speculated increased cell death, for example necrosis, apoptosis, autophagy and necroptosis, could play an essential role. In the HE staining of the peripheral pulmonary arteries, there were not obvious inflammatory response and vascular structure destruction, which excluded the occurrence of necrosis. Meanwhile, according to the results of immunohistochemical staining for LC3 and P62 in medial layer of pulmonary arteries, it suggested the level of autophagy didn't upregulate during reoxygenation. Necroptosis, as another important programmed cell death, doesn't depend on the caspase, which is different from apoptosis.[42] Importantly, the molecular pathway of necroptosis involves a different intermediate process, RIP-mediated signal transduction.[43] During reoxygenation, the expression of caspase–3 increased, and
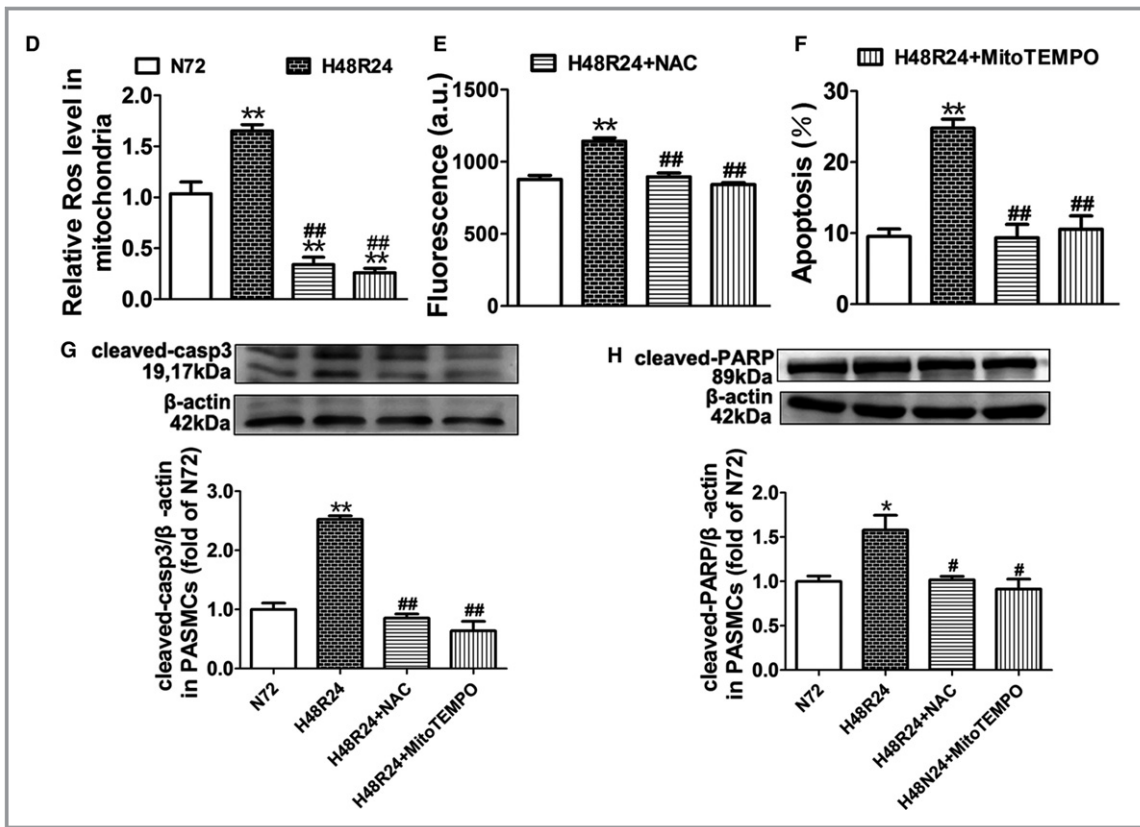
Figure 7. Continued.

the expression of RIP showed no significant change, which implied the level of necroptosis didn't increase. However, a previous study suggested that the reversal of pulmonary arterial remodeling was associated with increased apoptosis.[12] In this study, we further showed that the PASMCs apoptosis was induced during the reversal of pulmonary arterial remodeling, accompanied by increased H_2O_2. A study demonstrated that increased ROS could give rise to the PASMCs apoptosis.[19] These findings showed that PASMCs apoptosis participated in the reversal of hypoxic pulmonary arterial remodeling during reoxygenation, which might result from the increased ROS.

In vitro, our study demonstrated that the growth of cultured rat PASMCs accelerated markedly under hypoxia, consistent with the hypoxia-induced thickening of the pulmonary arterial medial layer.[44] Whether cultured PASMCs would show a similar regression process to that of the thickened medial layer during reoxygenaion was unknown. Our findings demonstrated a significant decrease in the growth of cultured PASMCs following hypoxia-reoxygenation, which might mimic the reversal of thickened medial layer in vitro. Actually, the growth of cells depends on the combined effects of apoptosis, nonapoptotic programmed cell death, and proliferation.[20] In our previous study, we did not find an increase of the nonapoptotic programmed cell death of PASMCs during reoxygenation, which implied that growth of PASMCs mainly depended on apoptosis and proliferation. The present study demonstrated that the apoptosis of cultured PASMCs increased significantly during reoxygenation, which broke the balance of PASMC growth.

As is widely known, large amounts of damaging ROS, mainly originating from mitochondria, are quickly generated following hypoxia-reoxygenation,[45-48] and the oxidative burst has been considered to play a crucial role in mediating the apoptosis of cells.[49,50] Our findings demonstrated that large amounts of mitochondrial ROS were generated in PASMCs during reoxygenation, which effectively promoted PASMC apoptosis. Apart from the main site of the mitochondrial ROS production, mitochondria are also important targets for the damaging effects of ROS. Therefore, mitochondrial regulation in cell death has drawn much attention recently.[51-53] Generally, large amounts of ROS could result in mitochondrial dysfunction, including mitochondrial permeability transition, inhibition of mitochondrial ATP production, and unbalance of Bcl-2-like survival factors and Bax-like death factors of Bcl-2 family proteins, which eventually trigger mitochondrial outer membrane permeabilization and give rise to the release of intermembrane proapoptosis factors.[21] This study
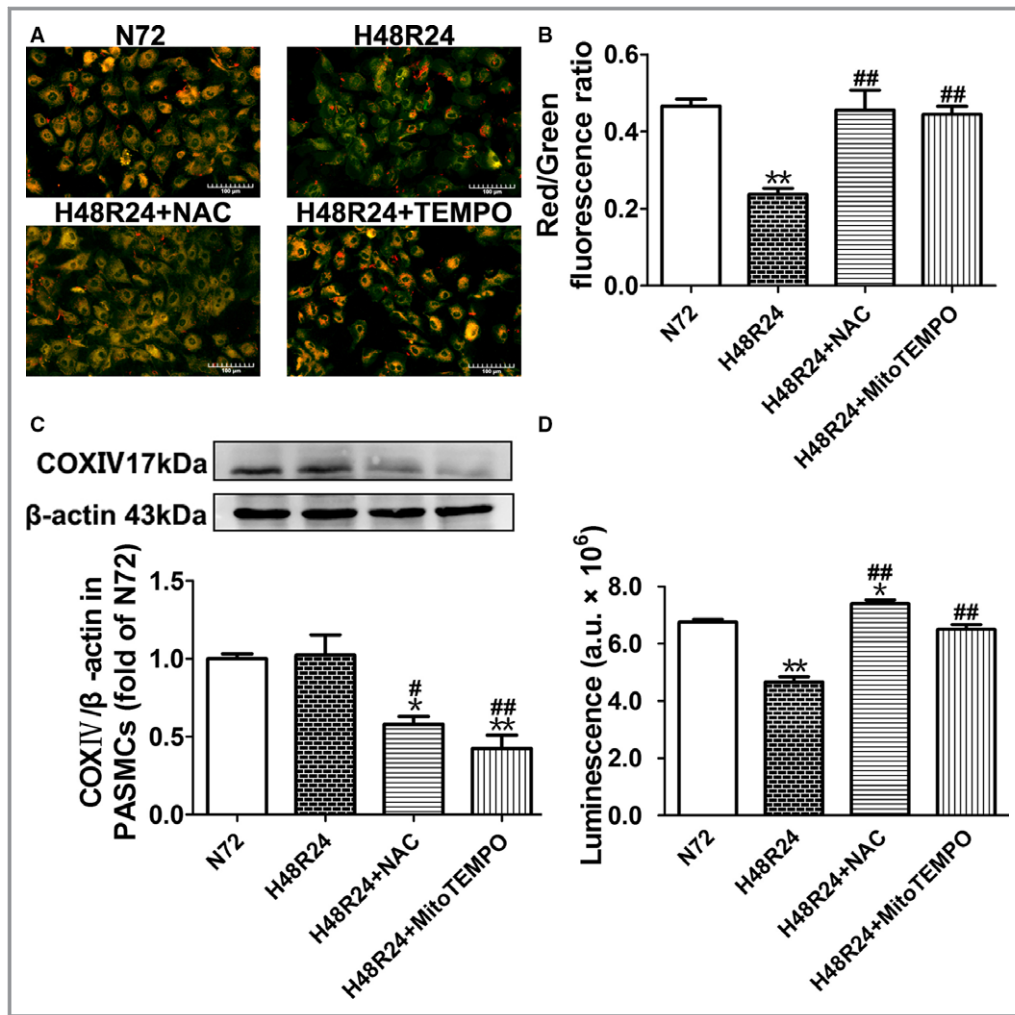
Figure 8. Mitochondrial reactive oxygen species (ROS) led to mitochondrial dysfunction during reoxygenation. Mitochondrial membrane potential of pulmonary arterial smooth muscle cells (PASMCs) ($>2\times10^4$ cells/coverslip), in the absence or presence of indicated antioxidants, was measured by confocal microscope with JC-1 staining (A). At $\times200$ magnification; Bar, 100 μm. Blinded quantitative analysis of red/green fluorescence ratios was performed (B). Mitochondrial content was relatively determined by the expression of COX-IV (cytochrome C oxidase IV) (C). Mitochondrial ATP production was assessed by the intensity of luminescence (D). Data are expressed as means±SEM (n=3 independent experiments). *$P<0.05$, **$P<0.01$ vs normoxia group; ##$P<0.01$ vs reoxygenation group by 1-way ANOVA with the Bonferroni posttest.

demonstrated that increased mitochondrial ROS damaged mitochondrial membrane potential and ATP production during reoxygenation and that these dysfunctions were alleviated by the clearance of mitochondrial ROS. The expression of Bax as well as the ratio of Bax/Bcl-2 also clearly increased during reoxygenation. Ultimately, the release of cytochrome C from the damaged mitochondria to cytoplasm increased significantly. These findings indicated that mitochondrial dysfunction, induced by excessive mitochondrial ROS, triggered PASMC apoptosis during reoxygenation.

However, after the intervention of MitoTEMPO (a mitochondria-directed antioxidant) in vivo, the reversal of RVSP,

MT, MA, and RV/(LV+Sep), which mainly depend on the effect of mitochondrial ROS, was not effectively inhibited during reoxygenation, which seemed to contradict the main observation of our manuscript. Unfortunately, maybe due to the much more complicated and unpredicted metabolism of MitoTEMPO in vivo, the H_2O_2 level of lung tissue in the R1+MitoTEMPO group showed no significant difference from that of R1 group, which might lead to the failure of MitoTEMPO to prevent the reversal of hypoxic pulmonary arterial remodeling. Therefore, we can not present more direct evidence to further consolidate the hypothesis in vivo. However, these could not deny that ROS, as the key factor,
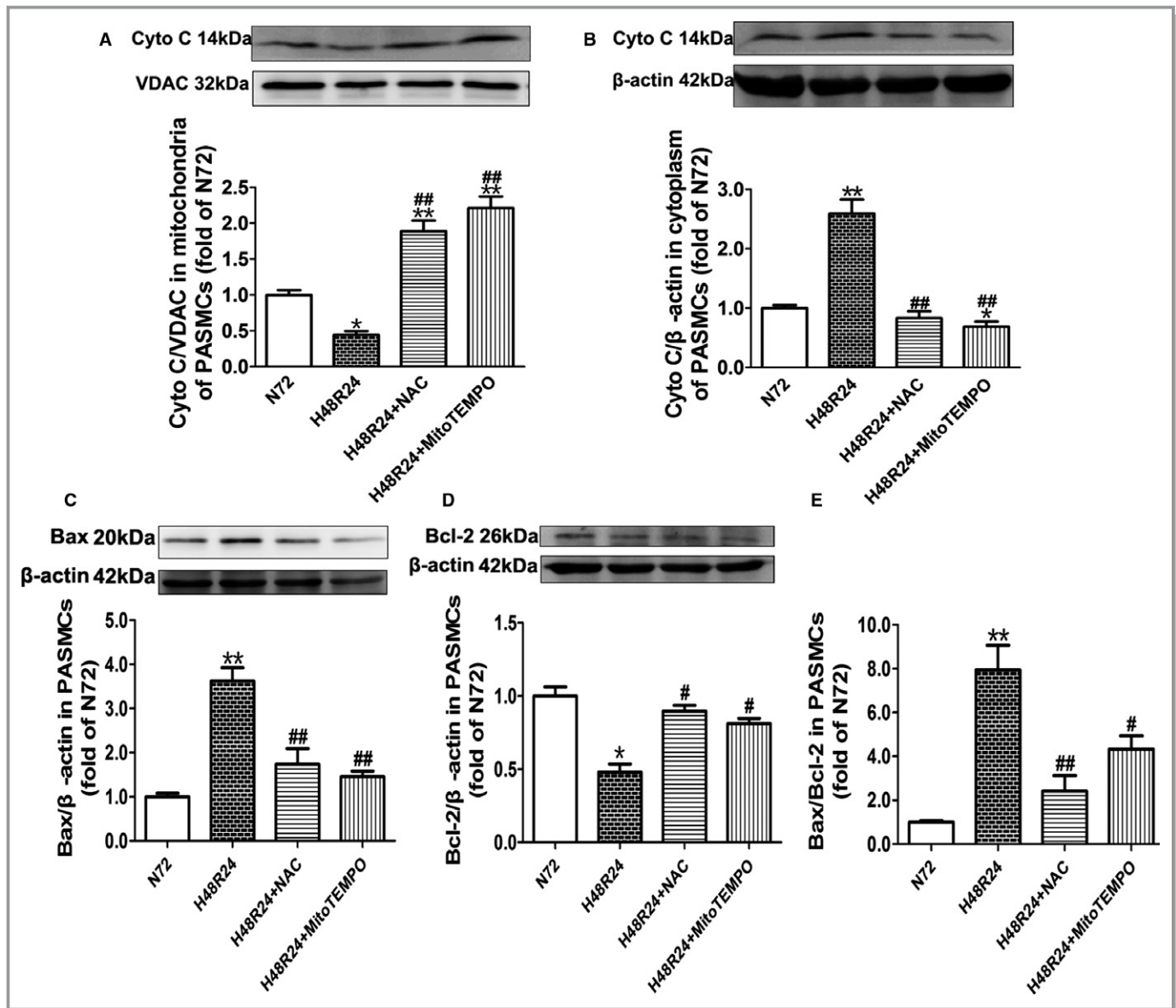
Figure 9. Mitochondrial reactive oxygen species (ROS) induced the release of cytochrome C from mitochondria to cytoplasm during reoxygenation. The distribution of cytochrome C in mitochondria (A) and cytoplasm (B) was analyzed through Western blotting with voltage–dependent anion channel (VDAC) and β-actin as internal control, respectively. The expressions of Bax (C) and Bcl-2 (D) in pulmonary arterial smooth muscle cells (PASMCs) ($>2\times10^6$ cells/sample), in the absence or presence of indicated antioxidants, was also determined with β-actin as an internal control. The protein ratio of Bax/Bcl-2 was demonstrated in Figure 8E. Data are normalized to the normoxia group and expressed as means±SEM (n=3 independent experiments). *$P<0.05$, **$P<0.01$ vs normoxia group; #$P<0.05$, ##$P<0.01$ vs reoxygenation group by 1-way ANOVA with the Bonferroni posttest.

initiated the reversal of hypoxic pulmonary arterial remodeling. Actually, there were large amounts of ROS generated in lung tissues during reoxygenation, and an important study had demonstrated that inducing the ROS burst could lead to the reversal of pulmonary arterial remodeling.[19] Moreover, we had demonstrated that the apoptosis of PASMCs increased significantly following hypoxia-reoxygenation in vitro, which resulted from the increased mitochondrial ROS.

Intriguingly, some studies reported that increased mitochondrial ROS, through various mechanisms, might finally lead to the apoptosis resistance of PASMCs during hypoxia,[54,55] and, for example, a study showed that increased ROS/mitochondrial ROS and dynamin-related protein-1 had a positive feedback loop that finally resulted in the apoptosis resistance of PASMCs by affecting the mitochondrial fission.[56] However, other studies showed that increased mitochondrial ROS could directly cause mitochondrial damage, resulting in the apoptosis of cells.[45,57] In this study, we demonstrated that excessive mitochondrial ROS was produced following hypoxia-reoxygenation, which directly
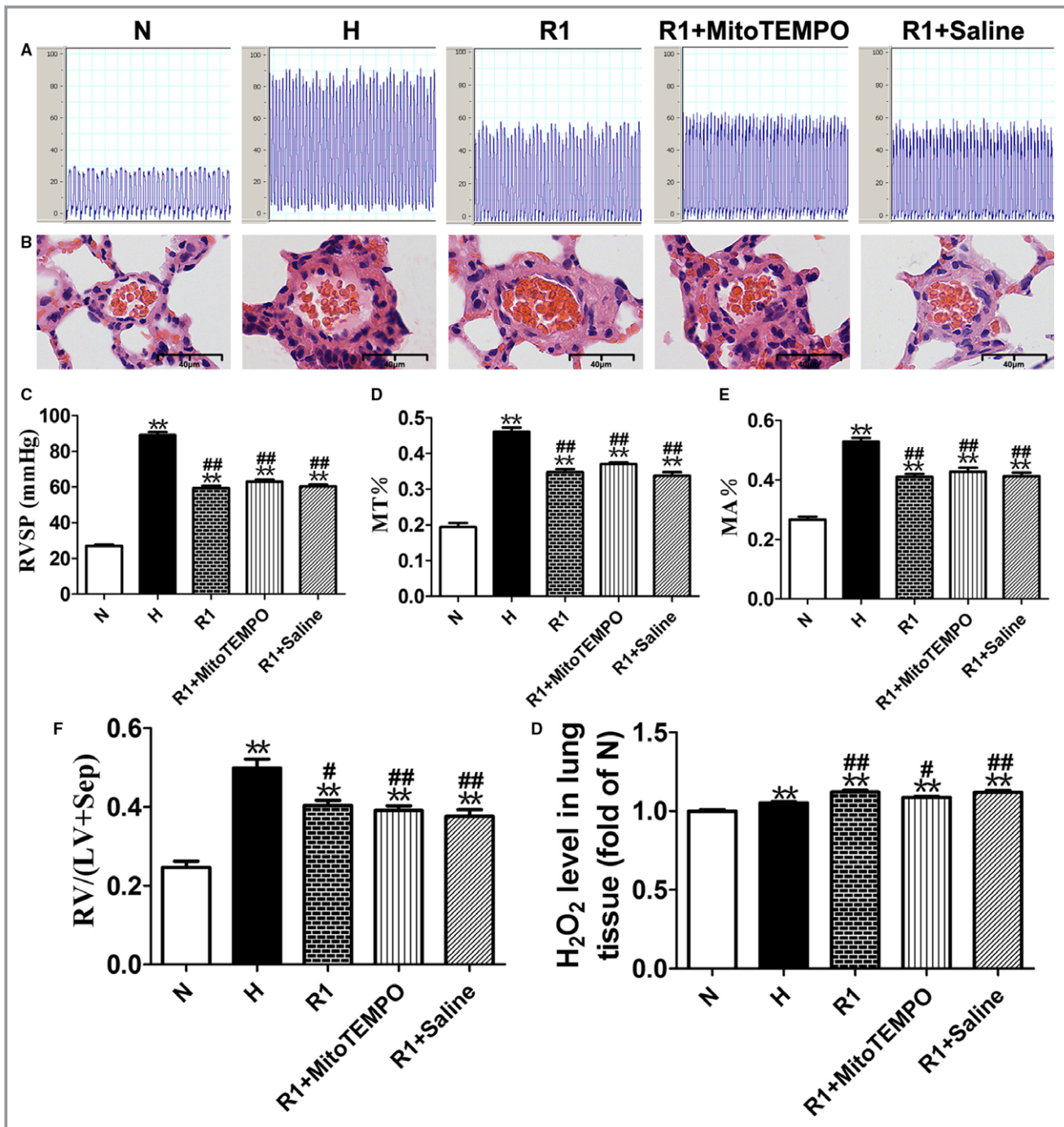
Figure 10. The intervention of MitoTEMPO failed to prevent the reversal of hypoxic pulmonary arterial remodeling in vivo. Representative images of right ventricle (RV) pressure traces and quantitative data of RV systolic pressure (RVSP) are shown (A and C). The paraffin sections of peripheral rat lungs were analyzed for pulmonary arterial remodeling through hematoxylin eosin staining (B). all at ×400 magnification; Bar, 40 µm. Blinded quantitative analysis of medial thickness (MT%) and medial area (MA%) of peripheral pulmonary arteries (30 vessels/3 sections of an animal, 30 to 100 µm in diameter) was performed with Image–Pro Plus (D and E). RV/(LV+Sep) and the level of H_2O_2 in lung tissues were shown in the bar charts (F and G). Data are presented as means±SEM (n=5-6 animals). **$P<0.01$ vs normoxia group; #$P<0.05$, ##$P<0.01$ vs hypoxia group by 1-way ANOVA with the Bonferroni posttest.

facilitated mitochondrial dysfunction and PASMC apoptosis. Although the effects of ROS/mitochondrial ROS on apoptosis were distinctly different, they all strikingly placed mitochondria at the center stage of apoptotic mechanisms. Practically, ROS/mitochondrial ROS present a characteristic threshold in inducing mitochondria-dependent apoptosis.[58] In

other words, ROS/mitochondrial ROS act as a common signaling molecule that becomes damaging only above a certain level. Therefore, further investigations are needed to determine the certain concentration of ROS, beyond which ROS will be a damaging factor.

In conclusion, our study raised awareness of reoxygenation-induced apoptosis of PASMCs, which may be triggered by mitochondrial ROS-mediated mitochondrial dysfunction, in the reversal of hypoxic pulmonary arterial remodeling. The present study provides a novel molecular insight into the mechanism of the reversal of hypoxic pulmonary arterial remodeling during reoxygenation.

Limitations

Several limitations of our study should be acknowledged. Because we only used male Sprague–Dawley rats in our study, it might be not enough to reflect the overall reversal of hypoxic pulmonary arterial remodeling during reoxygenation in rats. Moreover, the isolated rat PASMCs present a relatively high proliferation level in vitro, which may be inconsistent with the biological characteristics of the terminally differentiated PASMCs in vivo. Additionally, due to its combination with a cation triphenylphosphonium, the efficacy of MitoTEMPO closely depends on the mitochondrial membrane potential, which could enable MitoTEMPO to accumulate in mitochondria. Therefore, the function of mitochondria should be confirmed to be normal before MitoTEMPO is used as an antioxidant. Finally, one should also keep in mind the species difference and the limitation of chronically hypoxic rats as models of human pulmonary hypertension.

Sources of Funding

Disclosures

None.

References

1. Barberà JA, Peinado VI, Santos S. Pulmonary hypertension in chronic obstructive pulmonary disease. *Eur Respir J*. 2003;21:892–905.

2. Penaloza D, Arias-Stella J. The heart and pulmonary circulation at high altitudes: healthy highlanders and chronic mountain sickness. *Circulation*. 2007;115:1132–1146.

3. Wilkins MR, Ghofrani HA, Weissmann N, Aldashev A, Zhao L. Pathophysiology and treatment of high-altitude pulmonary vascular disease. *Circulation*. 2015;131:582–590.

4. Jeffery TK, Morrell NW. Molecular and cellular basis of pulmonary vascular remodeling in pulmonary hypertension. *Prog Cardiovasc Dis*. 2002;45:173–202.

5. Stenmark KR, McMurtry IF. Vascular remodeling versus vasoconstriction in chronic hypoxic pulmonary hypertension: a time for reappraisal? *Circ Res*. 2005;97:95–98.

6. Arias-Stella J, Saldana M. The terminal portion of the pulmonary arterial tree in people native to high altitudes. *Circulation*. 1963;28:915–925.

7. Abraham AS, Kay JM, Cole RB, Pincock AC. Haemodynamic and pathological study of the effect of chronic hypoxia and subsequent recovery of the heart and pulmonary vasculature of the rat. *Cardiovasc Res*. 1971;5:95–102.

8. Heath D, Edwards C, Winson M, Smith P. Effects on the right ventricle, pulmonary vasculature, and carotid bodies of the rat of exposure to, and recovery from, simulated high altitude. *Thorax*. 1973;28:24–28.

9. Hislop A, Reid L. Changes in the pulmonary arteries of the rat during recovery from hypoxia-induced pulmonary hypertension. *Br J Exp Pathol*. 1977;58:653–662.

10. Grover RF, Vogel JH, Voigt GC Jr, Blount SG. Reversal of high altitude pulmonary hypertension. *Am J Cardiol*. 1966;18:928–932.

11. Meyrick B, Reid L. Hypoxia-induced structural changes in the media and adventitia of the rat Hilar pulmonary artery and their regression. *Am J Pathol*. 1980;100:151–178.

12. Riley DJ, Thakker-Varia S, Wilson FJ, Poiani GJ, Tozzi CA. Role of proteolysis and apoptosis in regression of pulmonary vascular remodeling. *Physiol Res*. 2000;49:577–585.

13. Sluiter I, van Heijst A, Haasdijk R, Kempen MB, de Boerema-Munck A, Reiss I, Tibboel D, Rottier RJ. Reversal of pulmonary vascular remodeling in pulmonary hypertensive rats. *Exp Mol Pathol*. 2012;93:66–73.

14. Park HH, Lo YC, Lin SC, Wang L, Yang JK, Wu H. The death domain superfamily in intracellular signaling of apoptosis and inflammation. *Annu Rev Immunol*. 2007;25:561–586.

15. Thompson CB. Apoptosis in the pathogenesis and treatment of disease. *Science*. 1995;267:1456–1462.

16. Morrell NW, Adnot S, Archer SL, Dupuis J, Jones PL, MacLean MR, McMurtry IF, Stenmark KR, Thistlethwaite PA, Weissmann N, Yuan JX, Weir EK. Cellular and molecular basis of pulmonary arterial hypertension. *J Am Coll Cardiol*. 2009;54:S20–S31.

17. Cowan KN, Heilbut A, Humpl T, Lam C, Ito S, Rabinovitch M. Complete reversal of fatal pulmonary hypertension in rats by a serine elastase inhibitor. *Nat Med*. 2000;6:698–702.

18. Nishimura T, Vaszar LT, Faul JL, Zhao G, Berry GJ, Shi L, Qiu D, Benson G, Pearl RG, Kao PN. Simvastatin rescues rats from fatal pulmonary hypertension by inducing apoptosis of neointimal smooth muscle cells. *Circulation*. 2003;108:1640–1645.

19. McMurtry MS, Bonnet S, Wu X, Dyck JR, Haromy A, Hashimoto K, Michelakis ED. Dichloroacetate prevents and reverses pulmonary hypertension by inducing pulmonary artery smooth muscle cell apoptosis. *Circ Res*. 2004;95:830–840.

20. Fuchs Y, Steller H. Live to die another way: modes of programmed cell death and the signals emanating from dying cells. *Nat Rev Mol Cell Biol*. 2015;16:329–344.

21. Orrenius S, Gogvadze V, Zhivotovsky B. Mitochondrial oxidative stress: implications for cell death. *Annu Rev Pharmacol Toxicol*. 2007;47:143–183.

22. Holmstrom KM, Finkel T. Cellular mechanisms and physiological consequences of redox-dependent signalling. *Nat Rev Mol Cell Biol*. 2014;15:411–421.

23. Shimoda LA, Undem C. Interactions between calcium and reactive oxygen species in pulmonary arterial smooth muscle responses to hypoxia. *Respir Physiol Neurobiol*. 2010;174:221–229.

24. Wang W, Fang H, Groom L, Cheng A, Zhang W, Liu J, Wang X, Li K, Han P, Zheng M, Yin J, Wang W, Mattson MP, Kao JP, Lakatta EG, Sheu SS, Ouyang K, Chen J, Dirksen RT, Cheng H. Superoxide flashes in single mitochondria. *Cell*. 2008;134:279–290.

25. Chandra J, Samali A, Orrenius S. Triggering and modulation of apoptosis by oxidative stress. *Free Radic Biol Med*. 2000;29:323–333.

26. Ott M, Gogvadze V, Orrenius S, Zhivotovsky B. Mitochondria, oxidative stress and cell death. *Apoptosis*. 2007;12:913–922.

27. Li K, Cui YC, Zhang H, Liu XP, Zhang D, Wu AL, Li JJ, Tang Y. Glutamine reduces the apoptosis of h9c2 cells treated with high-glucose and reperfusion through an oxidation-related mechanism. *PLoS One*. 2015;10:e0132402.

28. Green DR, Galluzzi L, Kroemer G. Metabolic control of cell death. *Science*. 2014;345:1466.

29. Maiuri MC, Zalckvar E, Kimchi A, Kroemer G. Self-eating and self-killing: crosstalk between autophagy and apoptosis. *Nat Rev Mol Cell Biol*. 2007;8:741–752.

30. Luo Y, Xu DQ, Dong HY, Zhang B, Liu Y, Niu W, Dong MQ, Li ZC. Tanshinone IIA inhibits hypoxia-induced pulmonary artery smooth muscle cell proliferation via Akt/Skp2/p27-associated pathway. *PLoS One*. 2013;8:e56774.

31. Rabinovitch M, Gamble W, Nadas AS, Miettinen OS, Reid L. Rat pulmonary circulation after chronic hypoxia: hemodynamic and structural features. *Am J Physiol*. 1979;236:H818–H827.

32. Zimmer HG, Zierhut W, Seesko RC, Varekamp AE. Right heart catheterization in rats with pulmonary hypertension and right ventricular hypertrophy. *Basic Res Cardiol*. 1988;83:48–57.

33. Long L, Yang X, Southwood M, Lu J, Marciniak SJ, Dunmore BJ, Morrell NW. Chloroquine prevents progression of experimental pulmonary hypertension via inhibition of autophagy and lysosomal bone morphogenetic protein type II receptor degradation. *Circ Res*. 2013;112:1159–1170.

34. Phillips PG, Long L, Wilkins MR, Morrell NW. cAMP phosphodiesterase inhibitors potentiate effects of prostacyclin analogs in hypoxic pulmonary vascular remodeling. *Am J Physiol Lung Cell Mol Physiol*. 2005;288:L103–L115.

35. Zhang H, Gong Y, Wang Z, Jiang L, Chen R, Fan X, Zhu H, Han L, Li X, Xiao J, Kong X. Apelin inhibits the proliferation and migration of rat PASMCs via the activation of PI3K/Akt/mTOR signal and the inhibition of autophagy under hypoxia. *J Cell Mol Med*. 2014;18:542–553.

36. Korde AS, Yadav VR, Zheng YM, Wang YX. Primary role of mitochondrial Rieske iron-sulfur protein in hypoxic ROS production in pulmonary artery myocytes. *Free Radic Biol Med*. 2011;50:945–952.

37. Ma SH, Zhuang QX, Shen WX, Peng YP, Qiu YH. Interleukin-6 reduces NMDAR-mediated cytosolic Ca(2)(+) overload and neuronal death via JAK/CaN signaling. *Cell Calcium*. 2015;58:286–295.

38. Ramirez A, Grimes ET, Abelmann WH. Regression of pulmonary vascular changes following mitral valvuloplasty. An anatomic and physiologic case study. *Am J Med*. 1968;45:975–982.

39. Herget J, Suggett AJ, Leach E, Barer GR. Resolution of pulmonary hypertension and other features induced by chronic hypoxia in rats during complete and intermittent normoxia. *Thorax*. 1978;33:468–473.

40. Fried R, Reid LM. Early recovery from hypoxic pulmonary hypertension: a structural and functional study. *J Appl Physiol Respir Environ Exerc Physiol*. 1984;57:1247–1253.

41. Mouraret N, Marcos E, Abid S, Gary-Bobo G, Saker M, Houssaini A, Dubois-Rande JL, Boyer L, Boczkowski J, Derumeaux G, Amsellem V, Adnot S. Activation of lung p53 by Nutlin-3a prevents and reverses experimental pulmonary hypertension. *Circulation*. 2013;127:1664–1676.

42. Degterev A, Hitomi J, Germscheid M, Ch'En IL, Korkina O, Teng X, Abbott D, Cuny GD, Yuan C, Wagner G, Hedrick SM, Gerber SA, Lugovskoy A, Yuan J. Identification of RIP1 kinase as a specific cellular target of necrostatins. *Nat Chem Biol* 2008;4:313–321.

43. Mehta SL, Manhas N, Raghubir R. Molecular targets in cerebral ischemia for developing novel therapeutics. *Brain Res Rev*. 2007;54:34–66.

44. Yan J, Chen R, Liu P, Gu Y. Docosahexaenoic acid inhibits development of hypoxic pulmonary hypertension: in vitro and in vivo studies. *Int J Cardiol*. 2013;168:4111–4116.

45. Hernandez OM, Discher DJ, Bishopric NH, Webster KA. Rapid activation of neutral sphingomyelinase by hypoxia-reoxygenation of cardiac myocytes. *Circ Res*. 2000;86:198–204.

46. Braunersreuther V, Jaquet V. Reactive oxygen species in myocardial reperfusion injury: from physiopathology to therapeutic approaches. *Curr Pharm Biotechnol*. 2012;13:97–114.

47. Brown DI, Griendling KK. Regulation of signal transduction by reactive oxygen species in the cardiovascular system. *Circ Res*. 2015;116:531–549.

48. Korge P, Ping P, Weiss JN. Reactive oxygen species production in energized cardiac mitochondria during hypoxia/reoxygenation: modulation by nitric oxide. *Circ Res*. 2008;103:873–880.

49. Vakeva AP, Agah A, Rollins SA, Matis LA, Li L, Stahl GL. Myocardial infarction and apoptosis after myocardial ischemia and reperfusion: role of the terminal complement components and inhibition by anti-C5 therapy. *Circulation*. 1998;97:2259–2267.

50. Whelan RS, Kaplinskiy V, Kitsis RN. Cell death in the pathogenesis of heart disease: mechanisms and significance. *Annu Rev Physiol*. 2010;72:19–44.

51. Kroemer G, Galluzzi L, Brenner C. Mitochondrial membrane permeabilization in cell death. *Physiol Rev*. 2007;87:99–163.

52. Tait SW, Green DR. Mitochondria and cell death: outer membrane permeabilization and beyond. *Nat Rev Mol Cell Biol*. 2010;11:621–632.

53. Galluzzi L, Kepp O, Kroemer G. Mitochondria: master regulators of danger signalling. *Nat Rev Mol Cell Biol*. 2012;13:780–788.

54. Dromparis P, Sutendra G, Michelakis ED. The role of mitochondria in pulmonary vascular remodeling. *J Mol Med (Berl)*. 2010;88:1003–1010.

55. Guzy RD, Hoyos B, Robin E, Chen H, Liu L, Mansfield KD, Simon MC, Hammerling U, Schumacker PT. Mitochondrial complex III is required for hypoxia-induced ROS production and cellular oxygen sensing. *Cell Metab*. 2005;1:401–408.

56. Zhang LX, Ma C, Zhang C, Ma MF, Zhang FY, Zhang LL, Chen YL, Cao FY, Li SZ, Zhu DL. Reactive oxygen species effect PASMCs apoptosis via regulation of dynamin-related protein 1 in hypoxic pulmonary hypertension. *Histochem Cell Biol*. 2016;146:71–84.

57. Raat NJ, Shiva S, Gladwin MT. Effects of nitrite on modulating ROS generation following ischemia and reperfusion. *Adv Drug Deliv Rev*. 2009;61:339–350.

58. Dromparis P, Michelakis ED. Mitochondria in vascular health and disease. *Annu Rev Physiol*. 2013;75:95–126.